PHYSICAL REVIEW B VOLUME 28, NUMBER 11 1 DECEMBER 1983

Band theory of the magnetic interaction in MnO, MnS, and NiO

T. Oguchi and K. Terakura
Institute for Solid State Physics, University of Tokyo, Roppongi, Minato-ku, Tokyo 106, Japan

A. R. Williams
IBM Thomas J. Watson Research Center, Yorktown Heights, New York 10598
(Received 10 May 1983)

The interatomic coupling of magnetic moments in the insulating antiferromagnetic transition-metal compounds MnO, MnS, and NiO is calculated using a theory based on the itinerant-electron picture (energy-band theory and the local-spin-density treatment of exchange and correlation). Calculated values of these "Heisenberg" coupling constants agree with measured values to the extent that can be expected in light of the approximations required to execute the calculations. The calculations emphasize the importance of covalent interactions between the metal d states and the anion p states. These interactions are spin conserving and fundamentally nonmagnetic; they enter the coupling of the magnetic moments because the intra-atomic spin splitting of the metal d shell makes the covalent interactions dependent on the relative angle of the two magnetic moments.

I. INTRODUCTION

The transition-metal monoxides MnO, FeO, CoO, and NiO possess a special conceptual significance because the microscopic origin of their insulating nature[1-3] and antiferromagnetic ordering[4-6] has been and remains a fundamental, but unsettled, question of solid-state physics. While the insulating behavior of these substances is most often ascribed to the Mott-insulator mechanism, some attempts have also been made to interpret their behavior within the conceptual framework of single-particle energy-band theory.[7,8] In a recent paper[8] we showed that the insulating character of both MnO and NiO can be explained by purely band-structure effects, that is, without appeal to the Mott-insulator mechanism. Furthermore, the calculations in which the paramagnetic state above the Néel temperature was simulated by total spin disorder showed the local antiferromagnetic magnetization to be stable, even in the absence of long-range order for MnO.[9]

Whereas our previous paper was concerned primarily with the existence of a gap in the single-particle spectrum, the present work focuses on the extent to which the same itinerant-electron picture can also account for the interatomic coupling J of the magnetic moments as reflected, for example, in the spin-wave stiffness. The basic concept in this context is superexchange. Since the work by Kramers[4] many theoretical studies[5,10-16] have been made of the mechanism of superexchange. Anderson[6] gave an excellent review of the work through 1963 and developed a systematic theory of superexchange starting from the localized-orbital limit. In a qualitative sense, the theoretical background for the use of the Heisenberg model for the insulating magnets was established by Anderson's work. It has, however, proven very difficult to test the quantitative implications of Anderson's formulation by means of, for example, parameter-free calculations of the exchange coupling constants appropriate to a Heisenberg model[12-16] of spin-wave dynamics. Such calculations appear to be particularly difficult in the case of the transition-metal monoxides because the strength of the interaction (hybridization) between the transition-metal d orbitals and the oxygen p orbitals is so strong that a perturbative treatment starting from the localized-orbital limit is difficult, if not impossible.

For this reason, our approach starts from the opposite limit, that is, band theory. The method of analysis is an extension of our earlier work on iron.[17] It will be shown that the present band scheme can successfully explain qualitative features of the interatomic magnetic coupling J in MnO, MnS, and NiO, although the theoretical values of J are commonly about 3 times larger than the experimental values. (FeO and CoO are excluded from the present study because the effect of the unquenched orbital angular momentum cannot be treated properly within the present theoretical framework. On the other hand, MnS is included because of its similarity to MnO in several respects.) Because our analytical approach differs so pervasively from the traditional one, a precise one-to-one identification of the elements of our theory with the various superexchange mechanisms[6,4,15] is difficult. Furthermore, we believe that some of our results are qualitatively new. One new result is an interesting aspect of the role of the anion p orbitals in the magnetic interaction. Another is our finding that the ferromagnetic first-neighbor interaction in NiO results from d-band covalency, in contrast to the traditional approach where this effect is ascribed to potential exchange.[6]

The balance of the paper is organized as follows. In Sec. II we briefly describe the method of the calculation. Results are presented in Sec. III and discussed in Sec. IV. Section V is devoted to concluding remarks.

II. METHOD OF CALCULATION

We are concerned here with the change in total energy that results when the magnetic moment associated with an

TABLE I. Lattice constant a (in a.u.), Néel temperature T_N (in K), magnetic moment within the cation atomic sphere for the ground state, $M_{\rm loc}$(AF II), and for the paramagnetic state, $M_{\rm loc}$(para), and magnetic moment given by Eq. (5), M. $M_{\rm loc}$ and M are in units of μ_B.

	MnO	MnS	NiO
a	4.45	5.21	4.20
T_N	122	150	523
$M_{\rm loc}$(AF II)	4.46	4.39	1.05
$M_{\rm loc}$(para)	4.45	4.31	1.04
M	5.0	4.69	1.02

atom at position $\vec{R}_n$ is rotated relative to the moment associated with a reference atom at position $\vec{R}_0$. The particular estimate of this total-energy change that we are able to evaluate numerically is given by

$$\Delta E_n(\theta)=\frac{1}{\pi}\int^{\epsilon_F} d\epsilon\,\mathrm{Im}\ln\det[\mathbb{1}-K_0(\hat{e}_0)\tau^c_{0n}K_n(\hat{e}_n)\tau^c_{n0}]\ , \tag{1}$$

which is derived in Ref. 17. Equation (1) is based on two fundamental approximations: Firstly, the total-energy difference is approximated by the change in the sum of single-particle energies, and secondly, the moments in the neighborhood of the two atoms under consideration are assumed to be oriented in a completely random way. The latter is a convention for extracting the interaction energy between the particular two magnetic moments. The electronic structure of the medium of randomly oriented moments is described by the Korringa-Kohn-Rostoker coherent-potential approximation (KKR-CPA)[18] with the atomic-sphere approximation. The mathematical formulas for the individual quantities appearing in Eq. (1) can be found in Appendix A; we discuss here the simple physical picture embodied in Eq. (1). The two τ operators describe spin-conserving propagation in the medium of randomly oriented moments, while the K operators describe the single-site scattering by each of the two atoms under consideration. The scattering described by the K operators depends on the orientation of the spin of the individual electron, relative to the specified spin-quantization axis along the magnetic moment on each of the two atoms. The calculation consists of evaluating the total energy as a function of the relative angle θ of the two magnetic moment orientations $\hat{e}_0$ and $\hat{e}_n$ and as a function of the spatial separation of the two magnetically scattering atoms located at $\vec{R}_0$ and $\vec{R}_n$. Note, in particular, that it is primarily by means of the oxygen (or sulfur) p orbitals that the electrons propagate from one metal atom to another. This propagation, as well as propagation along other possible trajectories is described by the τ operators. We would like to point out that the tight-binding expression corresponding to Eq. (1) is equivalent to that of Ref. 19, which reduces to Anderson's kinetic superexchange[6] in the strong-correlation limit.[19,20]

The exchange interaction energy $E_n^{\rm ex}$ and the exchange parameter J_n are defined by

$$E_n^{\rm ex}=\tfrac{1}{2}[\Delta E_n(0)-\Delta E_n(\pi)] \tag{2}$$

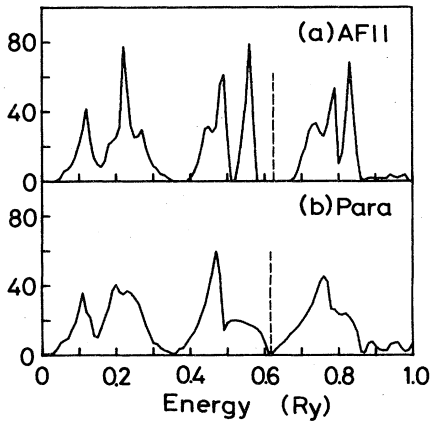

FIG. 1. Total state density of MnO (in states/Ry MnO) in (a) the antiferromagnetic state of the second kind, and (b) in the paramagnetic state. Vertical broken lines separate the occupied and unoccupied states.

and

$$J_n=-E_n^{\rm ex}/S^2\ . \tag{3}$$

The Heisenberg Hamiltonian appropriate to J_n defined in this way is

$$H=-\tfrac{1}{2}\sum_{i,n}J_n\vec{S}_i\cdot\vec{S}_{i+n}\ . \tag{4}$$

The quantity S appearing in Eq. (3) is $M/2$, where M is the magnitude of the spin magnetic moment per metal atom, which, in turn, is defined by

$$M=-\frac{1}{\pi}\mathrm{Im}\{\ln\det[\mathbb{1}-(t_c^{-1}-t_+^{-1})\tau^c_{00}] -\ln\det[\mathbb{1}-(t_c^{-1}-t_-^{-1})\tau^c_{00}]\}\ , \tag{5}$$

where t_c is the coherent t matrix and t_+ (t_-) is the single-site t matrix seen by an electron whose spin is parallel (antiparallel) to the orientation of the local magnetic moment on the site. (See Appendix A for further details.)

III. RESULTS

The calculations were performed for the observed lattice parameters. However, as the experimental data have some scatter, the lattice parameters we adopted are listed in Table I. The potentials used in the CPA calculations for the medium of randomly oriented moments (referred to hereafter as the paramagnetic state) were those obtained from the self-consistent augmented-spherical-wave (ASW) band calculations[8,21] for the ground-state antiferromagnetic ordering. Figures 1–3 show the total densities of states (DOS's) of MnO, MnS, and NiO in the paramagnetic and antiferromagnetic (second kind or "AF II") states. The results for MnO and NiO are the same as those presented in Ref. 8. In the ground state (AF II), the insulating gaps exist in all three substances, while only for MnO does the insulating gap persist in the paramagnetic state. In reali-

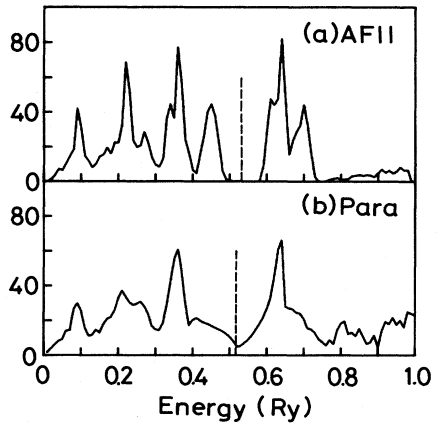

FIG. 2. Total state density of MnS (in states/Ry MnS) in (a) the antiferromagnetic state of the second kind, and (b) in the paramagnetic state. Vertical broken lines separate the occupied and unoccupied states.

ty, MnS and NiO are also insulators above the Néel temperature T_N. A weak aspect of our theory is the complete neglect of the short-range magnetic order in our model of the paramagnetic state. It is also true, of course that correlation effects beyond those described by the local-spin-density approximation may be unusually important in these systems. While our modeling of the paramagnetic state will limit the quantitative accuracy of estimates of the exchange coupling, we expect that the qualitative aspects of our results should not be affected.

The pair exchange interaction energy was calculated using Eqs. (1) and (2). It was found that $\Delta E_n(\theta)$ is almost exactly proportional to $\cos\theta$. The $\cos\theta$ dependence of $\Delta E_n(\theta)$ supports the use of the Heisenberg model of the form given by Eq. (4) and implies, as discussed in Appendix B, that Eq. (1) is well approximated by

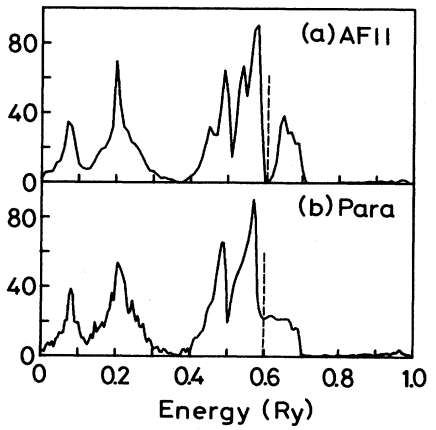

FIG. 3. Total state density of NiO (in states/Ry NiO) in (a) the antiferromagnetic state of the second kind, and (b) in the paramagnetic state. Vertical broken lines separate the occupied and unoccupied states.

TABLE II. Exchange interaction energies E_n^{ex} (in mRy) and exchange parameters J_n (in K).

	MnO		MnS		NiO	
n	E_n^{ex}	J_n	E_n^{ex}	J_n	E_n^{ex}	J_n
1	1.20	−30.3	0.37	−10	−0.10	61
2	1.18	−29.8	0.93	−27	2.02	−1230
3	0.0	0	0.00	0	0.02	−10
4	0.03	−0.8	0.03	−0.9	−0.12	73
5	0.02	−0.5	0.02	−0.6	−0.03	18
6	−0.01	0.3	0.01	−0.3	−0.01	6
7	−0.01	0.3	0.00	0	−0.01	6

$$\Delta E_n(\theta) = -\frac{1}{\pi}\int^{\epsilon_F} d\epsilon \,\mathrm{Im}\,\mathrm{Tr}[K_0(\hat{e}_0)\tau^c_{0n}K_n(\hat{e}_n)\tau^c_{n0}]\ , \tag{6}$$

where the trace operator Tr is taken over the space of angular momentum, site, and spin indices (L,n,s).

Next, we calculate the exchange parameters J_n using Eqs. (2), (3), and (5). Here, we comment on the values of S and M. In our band picture there is a distinction between the spin magnetic moment M given by Eq. (5) and that defined within the cation atomic sphere $M_{\rm loc}$. (In the localized orbital limit, the two quantities coincide.) The quantity $M_{\rm loc}$ in both the AF II state and the paramagnetic state are listed in Table I. The value of M given by Eq. (5) includes the tails of the magnetic polarization associated with a given cation and is the total magnetization that rotates simultaneously with the change in the direction of the cation magnetic moment. For MnO, which has an insulating gap even in the paramagnetic state, M is just 5. If an insulating gap also exists in paramagnetic MnS and NiO, M would be 5 (MnS) and 2 (NiO). Unfortunately, however, our model of complete disorder for the paramagnetic state does not produce a gap in MnS and NiO, and, as a result, the values of M given by Eq. (5) are 4.69 (MnS) and 1.02 (NiO). Although there is no rigorous justification, we use $M/2$ as S with M listed above. Table II shows the calculated exchange parameters J_n as well as the interaction energies E_n^{ex} up to the seventh neighbor for MnO, MnS, and NiO. A characteristic feature commonly seen in these three materials is that the exchange coupling between the first- and second-nearest neighbors is dominant, while the coupling between atoms more distant than second neighbor is much weaker, except for the fourth-neighbor coupling in NiO. The use of the spin Hamiltonian with the exchange parameters up to the second neighbor has been common in the analysis of the observed magnetic properties for these substances.[22–26] Our results provide justification for this type of approximation.

In the case of MnO, the first- and second-neighbor exchange coupling are both antiferromagnetic and have comparable magnitudes. As for MnS, the signs of the first- and second-neighbor coupling are the same as those in MnO, that is, both are antiferromagnetic, but the amplitude of the nearest-neighbor coupling is reduced to about half or less. On the other hand, some qualitatively different features are found in the exchange coupling of NiO. The nearest-neighbor coupling is weakly but defin-

TABLE III. Experimental and theoretical exchange parameters (in K) of the first and the second neighbors.

MnO		MnS		NiO		
J_1	J_2	J_1	J_2	J_1	J_2	Reference
−14.4	−7.0	−8.0	−9.0	−50	−85	22
−9.0	−10.4					25
				16	−222	26
−10.0	−11.0					23
−28	−28					24
−30.3	−29.8	−10	−27	61	−1230	present paper

itely ferromagnetic and the second-neighbor interaction is strongly antiferromagnetic, stronger than that for MnO and MnS. The latter feature is qualitatively consistent with the experimental observation that the Neél temperature T_N of NiO is about 5 times higher than that of MnO, as shown in Table I.

IV. DISCUSSION

A. Overall aspects

Consider now a comparison of the interatomic exchange interactions given by the present calculations with values deduced from experiment and estimates based on earlier theoretical work. Table III shows the exchange parameters derived from the analysis of the experimental data, such as thermodynamic quantities and spin-wave-dispersion data. As shown in Smart's review,[22] the molecular-field analysis for the Néel temperature and the susceptibility indicates a J_2/J_1 ratio of about 0.5, 1.0, and 1.7 for MnO, MnS, and NiO, respectively. It should be noted, however, that the molecular-field theory is known to overestimate the Néel temperature considerably. This was pointed out by Anderson[6] and by Lines and Jones.[23] It should also be noted that ambiguities exist in the experimental determination of the Weiss temperature due to the difficulty of the susceptibility measurements at high temperatures. An analysis of the thermodynamic quantities based on the Green's-function method[23] shows that the J_2/J_1 ratio for MnO lies very close to 1. A similar result was also obtained from the paramagnetic resonance measurement by Coles *et al.*[24] for Mn-pair impurities in MgO. Kohgi *et al.*[25] measured the spin-wave dispersion by neutron inelastic scattering at 4.2 K and found the J_2/J_1 ratio to be about 1.2 for MnO by fitting the effective spin Hamiltonian to the spin-wave-dispersion curve. Hutchings and Samuelson[26] found from the spin-wave measurements that the nearest-neighbor exchange coupling in NiO is smaller by an order of magnitude than the second-nearest-neighbor coupling and is ferromagnetic. The qualitative features exhibited by our calculated exchange couplings are fairly consistent with the experimental results listed above. However, our theory seems to overestimate the magnitude of the magnetic interaction, as shown in Table III. A possible reason of this quantitative disagreement is discussed in Sec. IV C.

Many theoretical efforts[4−6,10−16] have been made to elucidate the basic mechanisms in the superexchange interaction and to evaluate the exchange coupling constants quantitatively. Among these efforts, one of the most significant contributions is the Goodenough-Kanamori rule.[11,15] Briefly, the Goodenough-Kanamori rule states that if there is a finite transfer integral between orbitals of neighboring magnetic ions, then the antiferromagnetic kinetic superexchange dominates; if, on the other hand, the transfer is forbidden, then a weak ferromagnetic coupling due to the potential exchange is expected. Before discussing the results in Sec. III in a band picture we present a brief survey of the interpretation of the exchange interaction in MnO, MnS, and NiO given by the localized-orbital picture, mostly following Anderson.[6] In the case of MnO and MnS(d^5), the antiferromagnetic interaction of the second-nearest neighbor (180° coupling) is of kinetic exchange origin and is due mainly to the strong hybridization of Mn e_g with oxygen or sulfur p orbitals ($pd\sigma$-$pd\sigma$). The balance between the kinetic exchange of the $pd\pi$-$pd\pi$ type and potential exchange is believed to be weakly ferromagnetic. The nearest-neighbor coupling (90° coupling) for MnO and MnS is also antiferromagnetic due to the bond of t_{2g} orbitals of one Mn atom and e_g orbitals of the other via anion p orbitals ($pd\pi$-$pd\sigma$). As for NiO(d^8), the second-nearest-neighbor coupling is antiferromagnetic, and is again due to kinetic exchange of the $pd\sigma$-$pd\sigma$ type. It was argued that the antiferromagnetic coupling in NiO would be stronger than the corresponding coupling in MnO or MnS because the ferromagnetic potential exchange is absent in the d^8 case, whereas it makes an appreciable contribution in the d^5 case.[6] In the first-neighbor coupling (90° coupling) of NiO there is no kinetic exchange mediated by oxygen p orbitals. Since the kinetic exchange via the oxygen s orbital is expected to be very small, the net interaction will be weakly ferromagnetic, due to the potential exchange. The sign of the exchange interactions are all consistent with the Goodenough-Kanamori rule.[11,15]

We now describe the qualitative features of the exchange interaction as given by the band picture. The exchange energy ΔE_n of Eq. (1) is simply the sum of the change in the one-electron energies induced by the change in the relative angle of the two magnetic moments. By regarding ϵ_F as a variable parameter and plotting $E_n^{\rm ex}$ as a function of ϵ_F, we can see the change of the one-electron-energy sum in every energy range. This is the same fundamental idea that underlies our calculation of the nonlo-

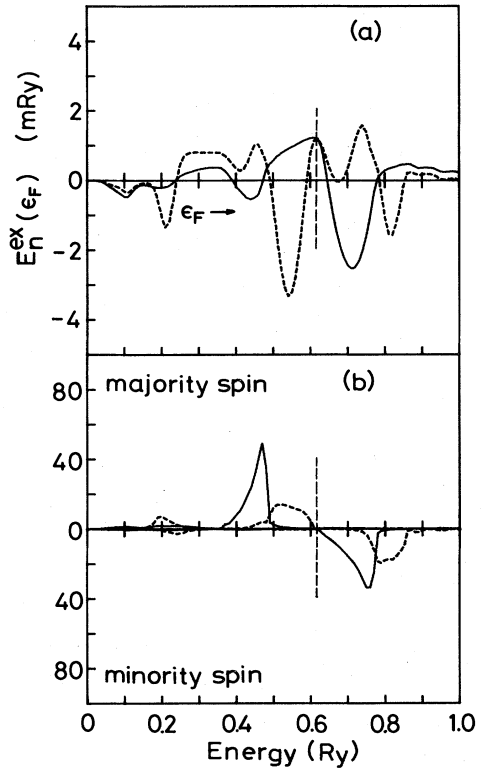

FIG. 4. (a) Exchange interaction energy E_n^{ex} for $n=1$ (solid line) and $n=2$ (broken line) as a function of ϵ_F, and (b) partial DOS's with e_g (solid line) and t_{2g} (broken line) symmetries at the Mn site for MnS. Vertical broken lines denote the actual Fermi energy.

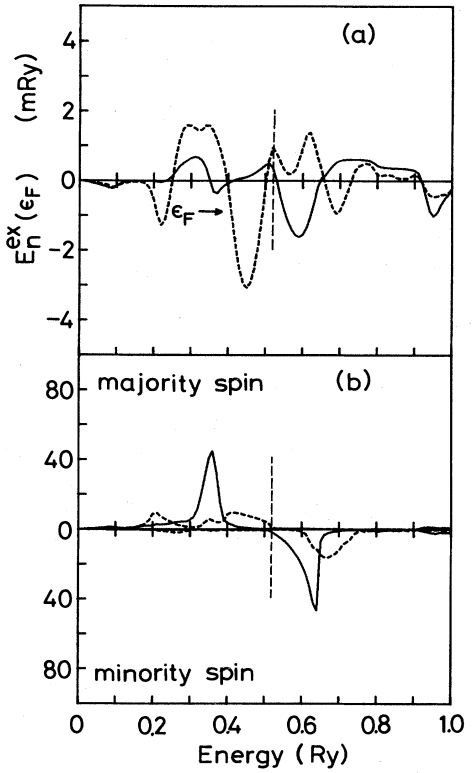

FIG. 5. (a) Exchange interaction energy E_n^{ex} for $n=1$ (solid line) and $n=2$ (broken line) as a function of ϵ_F, and (b) partial DOS's with e_g (solid line) and t_{2g} (broken line) as a function of ϵ_F, and (b) partial DOS's with e_g (solid line) and t_{2g} (broken line) symmetries at the Mn site for MnS. Vertical broken lines denote the actual Fermi energy.

cal susceptibility in transition metals.[27] In fact, Eq. (6) indicates that ΔE_n is essentially a nonlocal susceptibility of the paramagnetic state. Figures 4–6 show E_n^{ex} for $n=1$ and 2 as a function of ϵ_F and also the partial density of d states in MnO, MnS, and NiO. The relationship between the magnetic interaction and the filling of the d band, discussed by some workers for transition metals,[27–29] is basically valid in the present case also. For the case of a nearly-half-filled d band, the magnetic interaction between neighboring magnetic moments is generally antiferromagnetic, whereas when the d band is almost empty or almost filled, the interaction is ferromagnetic. An important point here is that the *inter*atomic magnetic coupling is communicated by d-band covalency effects,[30] which are not intrinsically magnetic; the coupling is not due to the electron-electron interaction. In the MnO and MnS cases, because the local majority-spin band is full and the local minority-spin band is empty, we can regard the band as a half-filled one in which the local spin subbands are split by the intra-atomic exchange energy. Therefore, the exchange interactions of the first and the second neighbors are antiferromagnetic. Figures 4 and 5 also show that the t_{2g} and e_g states play dominant roles in the first- and the second-neighbor exchange interactions, respectively, because $E_n^{ex}(\epsilon_F)$ varies strongly when ϵ_F falls in the energy regions where the corresponding subbands are located. Although the present approach looks different from the conventional kinetic exchange, the basic mechanism is the same. However, the energy denominator in the expression for the kinetic exchange in second-order perturbation theory is the exchange splitting of the d band in the present approach, whereas it is the Coulomb interaction itself in the localized-orbital picture.[6]

The situation for NiO is more complicated. We start our discussion with the second-neighbor coupling, which is determined by the covalency in the e_g subbands. Since the e_g subbands are half-filled, the second-neighbor coupling should be antiferromagnetic. We can also say that the coupling may be stronger than that in MnO and MnS because the exchange splitting is smaller, which may come into the energy denominator in the expression for the kinetic exchange in the second-order perturbation theory. With regard to the nearest-neighbor coupling the almost-filled t_{2g} subband produces a ferromagnetic coupling, but it is quite weak. The states above the Fermi energy consist primarily of e_g states, but small amount of t_{2g} states are also included because e_g and t_{2g} orbitals exhibit finite mixing in solids. We emphasize that the ferromagnetic coupling of the first-neighbor interaction is again due to

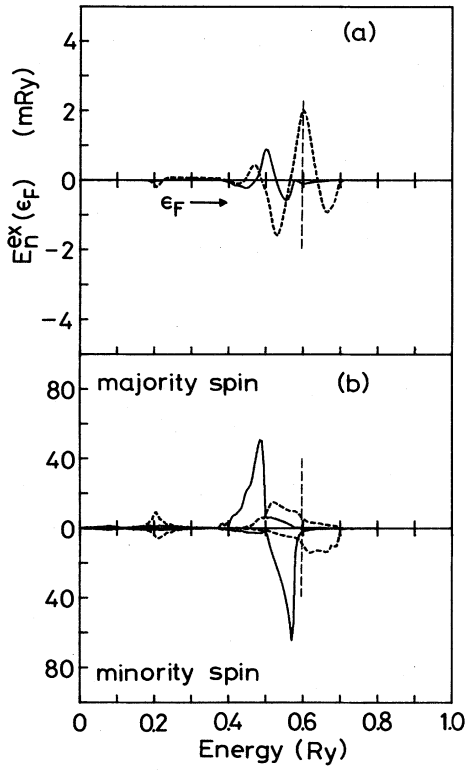

FIG. 6. (a) Exchange interaction energy E_n^{ex} for $n=1$ (solid line) and $n=2$ (broken line) as a function of ϵ_F, and (b) partial DOS's with e_g (solid line) and t_{2g} (broken line) symmetries at the Ni site for NiO. Vertical broken lines denote the actual Fermi energy.

d-band covalency in our band picture. This result differs qualitatively from the common understanding,[6] according to which potential exchange plays a role, as mentioned previously. The fact that our calculational model does not possess an energy gap in paramagnetic NiO, is almost certainly due to the absence of short-range magnetic order in the model of the paramagnetic state and not to any fundamental inadequacy of our band picture of the exchange coupling.

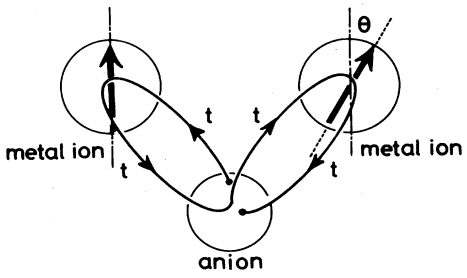

FIG. 7. Fourth-order contribution to the self-energy of the anion p states due to the p-d hybridization, which depends on the relative angle of the two magnetic moments surrounding an oxygen atom.

B. Role of the oxygen p states in the magnetic interaction

It should be noted in Figs. 4 and 5 that the exchange interaction $E_n^{ex}(\epsilon_F)$ is fairly large at the top of the anion p band in the case of MnO and MnS, which strongly affects $E_n^{ex}(\epsilon_F)$ at the actual Fermi energy. This means that the anion p bands make an appreciable contribution to the exchange interaction. It is the purpose of this subsection to clarify the role of the anion p states in the magnetic interaction. First, we note that the kinetic exchange in the second-order perturbation with regard to the effective hopping integral between metal atoms is fourth order with regard to the hybridization between the anion p and the metal d orbitals. In the following, we show that the dependence of the anion p-level shift on the magnetic alignment of the neighboring metal atoms is also fourth order in the p-d hybridization (see Fig. 7). The large value of $E_n^{ex}(\epsilon_F)$ just above the anion p state is explained by this effect.

Let us analyze the situation in Fig. 7 more explicitly. Consider a six-orthogonal-orbital (d—p—d bond) scheme. The atomic d level with majority (minority) spin, the atomic p level, and the p-d hybridization are denoted as $E_d-\Delta$ ($E_d+\Delta$), E_0, and t, respectively, where 2Δ is the exchange splitting of the d state. In order to calculate the lowest two molecular-orbital energies corresponding to the anion p band as a function of angle θ between the two moments, we solve the following secular equation:

$$\begin{vmatrix} E_d-\Delta-\epsilon & 0 & 0 & 0 & t & 0 \\ 0 & E_d+\Delta-e & 0 & 0 & 0 & t \\ 0 & 0 & E_d-\Delta\cos\theta-\epsilon & \Delta\sin\theta & t & 0 \\ 0 & 0 & \Delta\sin\theta & E_d+\Delta\cos\theta-\epsilon & 0 & t \\ t & 0 & t & 0 & E_0-\epsilon & 0 \\ 0 & t & 0 & t & 0 & E_0-\epsilon \end{vmatrix} = 0 . \tag{7}$$

After some manipulation, Eq. (7) is reduced to

$$(E_0-\epsilon)^2[(E_d-\epsilon)^2-\Delta^2]^2-4t^2(E_0-\epsilon)(E_d-\epsilon)[(E_d-\epsilon)^2-\Delta^2]+2t^4[2(E_d-\epsilon)^2-\Delta^2(1+\cos\theta)]=0 . \tag{8}$$

In Eq. (8) we postulate a solution of the form

$$\epsilon \sim E_0 - \xi t^2 + \eta t^4 - \cdots . \tag{9}$$

We substitute Eq. (9) into Eq. (8), and solve for ξ and η, obtaining

$$\xi_{\pm} = \frac{2(E_d - E_0) \pm \Delta \cos(\theta/2)}{(E_d - E_0)^2 - \Delta^2} , \tag{10}$$

$$\eta_{\pm} = \frac{2\xi_{\pm}[\xi_{\pm}(E_d - E_0) - 1]}{(E_d - E_0)^2 - \Delta^2} . \tag{11}$$

Then, the sum of the energy shifts of p levels due to the p-d hybridization is given by

$$\begin{aligned} \Delta E &= -(\xi_+ + \xi_-)t^2 + (\eta_+ + \eta_-)t^4 \\ &= -\frac{4(E_d - E_0)}{(E_d - E_0)^2 - \Delta^2} t^2 \\ &\quad + \frac{8(E_d - E_0)[(E_d - E_0)^2 + \Delta^2(2 + \cos\theta)]}{[(E_d - E_0)^2 - \Delta^2]^3} t^4 . \end{aligned} \tag{12}$$

In Eq. (12), it is natural that the t^2 term does not depend on θ because it has no path connecting the different metal atoms. The anion p-state contribution to the exchange energy is found to be

$$\begin{aligned} E_{\text{ex}}^{\text{anion}} &= \tfrac{1}{2}[\Delta E(\theta = 0) - \Delta E(\theta = \pi)] \\ &= \frac{8(E_d - E_0)\Delta^2}{[(E_d - E_0)^2 - \Delta^2]^3} t^4 . \end{aligned} \tag{13}$$

The contribution is antiferromagnetic for the present band parameters and is proportional to Δ^2 as expected.

Now we consider specific coupling schemes for the first and second neighbors. The former is a 90° bond case, in which, for example, two metal atoms are situated at $a(0,0,\frac{1}{2})$ and $a(\frac{1}{2},0,0)$ and an anion atom at the origin. The latter is a 180° case, in which for example, the bond axis is directed in the z direction. In the 90° case, as the fourth-order hopping between different metal atoms occurs via the anion, there are three paths,

$$d_{3z^2-r^2} - p_z - d_{zx}, \quad d_{zx} - p_x - d_{3x^2-r^2}, \quad d_{yz} - p_y - d_{xy} . \tag{14}$$

Then, t^4 in Eq. (13) is expressed as

$$(t^4)_1 = 2(pd\sigma)^2(pd\pi)^2 + (pd\pi)^4 \tag{15}$$

using the tight-binding parameters. In the 180° case, the following three fourth-order hopping paths exist:

$$d_{3z^2-r^2} - p_z - d_{3z^2-r^2}, \quad d_{zx} - p_x - d_{zx}, \quad d_{yz} - p_y - d_{yz} . \tag{16}$$

Then, t^4 is expressed as

$$(t^4)_2 = (pd\sigma)^4 + 2(pd\pi)^4 . \tag{17}$$

By using Mattheiss's hopping parameters, $pd\sigma \sim -0.0737$ Ry and $pd\pi \sim 0.0318$ Ry, for MnO (Ref. 31) we get a ratio $(t^4)_2/(t^4)_1$ of 2.7, where we have neglected, for simplicity, the overlap integrals between the d and p orbitals, which were included in Mattheiss's parameters. The anion p contribution of the second neighbor is more than twice as large as that of the first neighbor in MnO, which is consistent with the behavior of E_n^{ex} at $\epsilon_F \sim 0.3$ Ry in Fig. 4(a). If we use the band parameters, $(E_d - E_0) \sim 0.45$ Ry and $\Delta \sim 0.14$ Ry, for MnO, which are taken from the band structure in the CPA calculation, then the magnitude of the anion p contribution is a few tenths of a mRy. In MnS the contribution may be larger than that in MnO, because $E_d - E_0$ is smaller and the hopping integrals are larger. In NiO the contribution is considerably smaller because of the small exchange splitting ($\Delta \sim 0.04$ Ry). In this way the features pointed out at the beginning of the section are successfully explained. The mechanism discussed above has some similarity to Slater's mechanism,[10,14] in which the polarization of the anion states plays a role through the admixture of the $3s$ state into the $2p$ states.

We now proceed one step further. One might expect that $E_n^{\text{ex}}(\epsilon_F)$ in Figs. 4–6 would be proportional to Δ^2 for any value of ϵ_F and then the Δ^2 dependence of $E_{\text{ex}}^{\text{anion}}$ in Eq. (13) cannot explain the fact that $E_{\text{ex}}^{\text{anion}}$ is important in MnO and MnS, but less important in NiO. The point in this regard is that $E_n^{\text{ex}}(\epsilon_F)$ for ϵ_F in the d-band region is proportional to Δ rather than to Δ^2 because Δ comes into the energy denominator in the perturbation treatment of the covalency effect in the d band. Therefore, the contribution of $E_{\text{ex}}^{\text{anion}}$ to the exchange coupling becomes relatively important when Δ is large.

C. Origins of the overestimate of exchange coupling

We compare the results of the exchange interaction with the total energy of ordered MnO and MnS. As presented in another paper,[21] we calculated the total energies of MnO and MnS in the three magnetic configurations: ferromagnetic and two antiferromagnetic orderings, the first kind (AF I) and the second kind (AF II). The total energy of AF II is lower than that of AF I by 5.4 mRy for MnO and 5.7 mRy for MnS, which is consistent with the experimentally observed AF II ordering. Assuming that the energy difference is described by the effective-pair spin Hamiltonian with the exchange interaction obtained in this work, we obtain 4.4 mRy for MnO and 5.1 mRy for MnS. Although the agreement between the results from the two different approaches is quite satisfactory, it may be accidental and perhaps we cannot expect more than the fact that the results obtained using the two approaches are the same order of magnitude.

We comment briefly on the possible origins of the overestimate by the present calculation of the interatomic exchange coupling. For NiO the present band calculation underestimates the magnetic moment and therefore the exchange splitting. This leads to a serious overestimate of the interatomic exchange coupling. The same may also be true for MnO and MnS, although with less significance. Other possible origins for the overestimation are conceivable. For example, the present prescription for evaluating the exchange coupling takes account of only the band-

energy term. Generally speaking, the screening effect by the electron-electron interaction reduces the change in the band-energy contribution. However, the fact that the ASW result also overestimates the magnetic energy difference seems to suggest that this screening effect may not be so important because the ASW calculation takes account of the screening effect within the local spin-density-functional (LSDF) formalism. Of course, this counterproof based on the importance of the screening effect has some ambiguities. As the two magnetic configurations, the first and the second kinds of antiferromagnetic orderings are quite different from each other and the state densities for them, for example, are also quite different (see Fig. 2 in Ref. 8). Therefore, the basic assumption that the energy difference between the two magnetic orderings is described by the pair interactions is questionable. A third possibility is the nonsphericity of the intra-atomic potential. Neutron scattering[32] shows that the magnetic distribution around Ni in NiO, for example, has appreciable nonsphericity. Both the ASW calculation and our CPA calculation do not take into account the nonsphericity of the potential at all. A possible way of studying the effect of insufficiency of these methods in treating the potential is to change the atomic radius for each constituent atom. Recently, Kübler studied how the total energy depends on the choice of atomic radii.[33] He changed the ratio of the Mn and O radii $r=R_{\mathrm{Mn}}/R_{\mathrm{O}}$ from 1.18 to 0.75. A value of $r=1.18$ is approximately the same as that used in the present work, obtained using a prescription based on the bulk moduli of the constituent elemental materials. The value $r=0.75$, on the other hand, is close to the ratio of the ionic radii for $Mn^{2+}O^{2-}$. Kübler found that the total-energy difference between the first and the second antiferromagnetic orderings changes from 5.9 mRy ($r=1.18$) to 3.5 mRy ($r=0.75$). The fact that such a gross change in the atomic decomposition of the unit cell causes the total energy to change so little is encouraging, but it is also true that the total-energy differences of interest in the present context are also very small; Kübler's sensitivity test is an indication of the desirability of treating the shape of the potential more accurately. As the energy scale of interest is very small, there may be other possibilities for the error in the numerical computation. The refinement of the numerical accuracy is one of the future tasks.

V. CONCLUDING REMARKS

Energy-band theory was applied to the calculation of the superexchange interaction in MnO, MnS, and NiO. These materials are usually regarded as Mott insulators. It was pointed out that the band calculation accounts well for the insulating behavior of these substances.[8,21] The present calculation is based on the KKR CPA calculations for the paramagnetic state where each cation atom has a finite magnetic moment with random orientation. Our approach successfully explains the qualitative features of the exchange interactions. Our interpretation of the exchange interaction in NiO has some qualitative differences from the traditional one, which is based on the localized-orbital picture.[6] It was also pointed out that the shift of the anion p level due to the p-d hybridization depends on the magnetic alignment of the neighboring cation atoms and that this makes a fairly large contribution to the superexchange interaction for MnO and MnS. However, the exchange interaction is on the order of mRy, which makes a quantitative agreement quite difficult. The present scheme overestimates the exchange interactions for MnO, MnS, and NiO by a factor of about 3. Possible origins of this disagreement were discussed.

ACKNOWLEDGMENTS

This work was initiated while one of the authors (K.T.) was a visiting scientist at the IBM Thomas J. Watson Research Center. He would like to express his sincere thanks to the IBM World Trade Corporation for supporting his stay there. Useful advice from Dr. N. Hamada on the convergence problem of the CPA self-consistent equation is acknowledged. Thanks are also given to Professor Dr. J. Kübler for valuable comments. This work was supported in part by a Grant-in-Aid for Cooperative Research from the Ministry of Education, Science and Culture of Japan. The numerical computation was done mostly with the M-200H computer at the Institute for Molecular Science.

APPENDIX A: BRIEF SUMMARY OF THE KKR CPA FOR DERIVING EQ. (1)

The KKR CPA was applied to describe the electronic structure of the system in which the magnetic moment at each atom is oriented randomly. The procedure for obtaining Eq. (1) is essentially the same as that in our work on iron,[17] which should be referred to for the detailed prescription. In this appendix we give explicit expressions of the quantities appearing in Eq. (1) and also point out some small differences between the present calculation for compounds and the previous one for the element iron.

In Eq. (1), $\hat{e}_0$ ($\hat{e}_n$) is the direction of the magnetic moment at $\vec{R}_0$ ($\vec{R}_n$) and K and t^c are given by

$$K_0(\hat{e}_0)=[1-(t_c^{-1}-t^{-1})_{00}\tau^c_{00}]^{-1}(t_c^{-1}-t^{-1})_{00} \tag{A1}$$

and

$$\tau^c=(t_c^{-1}-G)^{-1}\ . \tag{A2}$$

t_c is the coherent t matrix, t is the single-site t matrix, and G is the structural Green's function. The quantities denoted by τ are matrices in the space spanned by (L,n,s) where L denotes the orbital angular momentum (l,m), n denotes the lattice site, and s denotes the spin state. The matrix elements of these quantities with regard to lattice sites are

$$(t)_{nn'}=t_n\delta_{nn'}\ , \tag{A3}$$

$$(t_c)_{nn'}=t_{c,n}\delta_{nn'}\ , \tag{A4}$$

$$(K)_{nn'}=K_n(\hat{e}_n)\delta_{nn'}\ , \tag{A5}$$

and

$$(\tau^c)_{nn'}=\tau^c_{nn'}\delta_{nn'}\ . \tag{A6}$$

We note that the anion sublattice has the perfect periodicity and $t_{c,n}$ is just t_n, the t matrix for the anion potential if $\vec{R}_n$ is an anion site. Therefore, the effect of the anion sublattice enters into ΔE_n through τ^c in Eq. (A2). With this in mind we regard the indices 0, n, and n' in Eqs. (1) and (A1)—(A6) as the site indices in the cation sublattice. Then $t_{c,n}$ in Eq. (A4) is independent of n. By using the 2×2 unit matrix $\mathbb{1}$ and Pauli matrices σ_x, σ_y, and σ_z, t_n is expressed as

$$t_n=\tfrac{1}{2}(t_+ +t_-)\times\mathbb{1}+\tfrac{1}{2}(t_+ -t_-)\times(\hat{e}_n\cdot\vec{\sigma}) , \tag{A7}$$

where $\vec{\sigma}$ is a vector spanned by the Pauli matrices and t_+ (t_-) is the t matrix "seen" by an electron whose spin is parallel (antiparallel) to $\hat{e}_n$. The transition matrices t_+ and t_- are matrices spanned by L and are common to all cation sites (t^+, t^-, t_c, K_+, K_-), and τ^c_{00} are diagonal in L space so long as $l\leq 2$. The multiplication sign in Eq. (A7) indicates a direct product between the matrix in the orbital space and that in the spin space. The quantity K is also expressed similarly. [See Eq. (18) in Ref. 17 and Eqs. (B2) and (B3) in Appendix B.] τ^c as well as t_c and G is diagonal in spin space and expressed as

$$\tau^c=\tau^c\times\mathbb{1} , \tag{A8}$$

where τ^c is a matrix spanned by (L,n).

The CPA self-consistency equation for the determination of t_c is

$$\int d\Omega\, K_0(\hat{e}_0)=0 , \tag{A9}$$

where the integration is over the orientation of $\hat{e}_0$. By using Eq. (B2) from Appendix B, Eq. (A9) is reduced to

$$K^+ +K^-=0 , \tag{A10}$$

or more explicitly,

$$t_c^{-1}=\tfrac{1}{2}(t_+^{-1}+t_-^{-1})+(t_c^{-1}-t_+^{-1})\tau^c_{00}(t_c^{-1}-t_-^{-1}) , \tag{A11}$$

which is the CPA equation for the system where the local magnetic moments take only up or down orientation randomly.

We comment on technical aspects of the CPA calculation. As the d band is fairly narrow in transition-metal oxides, the convergence of the iterative solution of the CPA equation (A11) is generally slow. Ducastelle[34] discussed this convergence problem and proposed a useful solution, which we adopted in the present work: By using the averaged t matrix as a starting t_c, an approximate coherent t matrix in the ith iteration $t_c^{(i)}$ is used to obtain t_c of the next step by

$$(t_c^{(i+1)})^{-1}=(t_c^{(i)})^{-1}-\langle K^{(i)}\rangle(\mathbb{1}+\langle K^{(i)}\rangle\tau^{c(i)}_{00})^{-1} , \tag{A12}$$

with

$$\langle K^{(i)}\rangle\equiv\tfrac{1}{2}(K^{+(i)}+K^{-(i)}) . \tag{A13}$$

APPENDIX B: $\cos\theta$ DEPENDENCE OF ΔE OF EQ. (1)

We make use of the following equation:

$$\ln\det(\mathbb{1}+A)=\mathrm{Tr}A+\mathrm{Tr}A^2+\tfrac{1}{2}(\mathrm{Tr}A)^2+\cdots . \tag{B1}$$

If we retain the first-order term, Eq. (1) is reduced to Eq. (6). Like Eq. (A7), the K matrix is also expressed as

$$K_0(\hat{e}_0)=\tfrac{1}{2}(K^+ +K^-)\times\mathbb{1}+\tfrac{1}{2}(K^+ -K^-)\times(\hat{e}_0\cdot\vec{\sigma}) , \tag{B2}$$

$$K_n(\hat{e}_n)=\tfrac{1}{2}(K^+ +K^-)\times\mathbb{1}+\tfrac{1}{2}(K^+ -K^-)\times(\hat{e}_n\cdot\vec{\sigma}) . \tag{B3}$$

With Eqs. (A8), (B2), and (B3), we obtain

$$\begin{aligned}K_0(\hat{e}_0)\tau^c_0K_n(\hat{e}_n)\tau^c_{n0}=&\tfrac{1}{4}[(K^+ +K^-)\tau^c_{0n}(K^+ +K^-)\tau^c_{n0}]\times\mathbb{1}+\tfrac{1}{4}[(K^+ -K^-)\tau^c_{0n}(K^+ +K^-)\tau^c_{n0}]\times(\hat{e}_0\cdot\vec{\sigma})\\&+\tfrac{1}{4}[(K^+ +K^-)\tau^c_{0n}(K^+ -K^-)\tau^c_{n0}]\times(\hat{e}_n\cdot\vec{\sigma}+\tfrac{1}{4}[(K^+ -K^0)\tau^c_{0n}(K^+ -K^-)\tau^c_{n0}]\\&\times[(\hat{e}_0\cdot\hat{e}_n)\mathbb{1}+i(\hat{e}_0\times\hat{e}_n)\cdot\vec{\sigma}] ,\end{aligned} \tag{B4}$$

where we make use of the relation

$$(\hat{e}_0\cdot\vec{\sigma})(\hat{e}_n\cdot\vec{\sigma})=(\hat{e}_0\cdot\hat{e}_n)\mathbb{1}+i(\hat{e}_0\times\hat{e}_n)\cdot\vec{\sigma} . \tag{B5}$$

The trace of (B4) over (L,n,s) is reduced to

$$\mathrm{Tr}[K_0(\hat{e}_0)\tau^c_{0n}K_n(\hat{e}_n)\tau^c_{n0}]=\tfrac{1}{2}\{\mathrm{Tr}[(K^+ +K^-)\tau^c_{0n}]^2+\mathrm{Tr}[(K^+ -K^-)\tau^c_{0n}]^2\cos\theta\} , \tag{B6}$$

where θ is the angle between $\hat{e}_0$ and $\hat{e}_n$ and Tr on the right-hand side of Eq. (B6) is over (L,n). Therefore, the $\cos\theta$ dependence of Eq. (1) implies that the first term in (B1) dominates. This implies also that the many spin interactions beyond the pair interaction in Eq. (4) can be neglected.

[1]N. F. Mott, Proc. Phys. Soc. London Sect. A 62, 416 (1949).
[2]D. Adler, in *Solid State Physics,* edited by F. Seitz and D. Turnbull (Academic, New York, 1968), Vol. 21, p.1.
[3]B. H. Brandow, Adv. Phys. 26, 651 (1977).
[4]H. A. Kramers, Physica (Utrecht) 1, 182 (1933).
[5]P. W. Anderson, Phys. Rev. 115, 2 (1959).
[6]P. W. Anderson, in *Solid State Physics,* edited by F. Seitz and D. Turnbull (Academic, New York, 1963), Vol. 14, p. 99.
[7]T. M. Wilson, Int. J. Quant. Chem. Symp. 3, 757 (1970).
[8]K. Terakura, T. Oguchi, A. R. Williams, and J. Kübler (unpublished).
[9]The band calculations were done with the ASW method [A. R. Williams, J. Kübler, and C. D. Gelatt, Jr., Phys. Rev. B 19, 6094 (1979)] and the paramagnetic calculations were done with the atomic-sphere CPA.
[10]J. C. Slater, Quarterly Progress Report Massachusetts Institute of Technology, July 15,1; Oct. 15,1 (1953) (unpublished).
[11]J. B. Goodenough, Phys. Rev. 100, 564 (1955).
[12]R. K. Nesbet, Ann. Phys. 4, 87 (1958); Phys. Rev. 119, 658 (1960).
[13]J. Kondo, Prog. Theor. Phys. 18, 541 (1957).
[14]J. Yamashita and J. Kondo, Phys. Rev. 109, 730 (1958).
[15]J. Kanamori, J. Phys. Chem. Solids 10, 87 (1959).
[16]F. Keffer and T. Oguchi, Phys. Rev. 115, 1428 (1959).
[17]T. Oguchi, K. Terakura, and N. Hamada, J. Phys. F 13, 145 (1983).
[18]B. L. Györffy and G. M. Stocks, in *Electrons in Disordered Metals and Metallic Surfaces,* edited by P. Phariseau, B. L. Györffy, and L. Scheire (Plenum, New York, 1979), p. 89.
[19]P. Lacour-Gayet and M. Cyrot, J. Phys. C 7, 400 (1974).
[20]T. Moriya and H. Hasegawa, J. Phys. Soc. Jpn. 48, 1490 (1980).
[21]T. Oguchi, K. Terakura, A. R. Williams, and J. Kübler (unpublished).
[22]J. S. Smart, in *Magnetism,* edited by G. T. Rado and H. Suhl (Academic, New York, 1963), Vol. 3, p. 63.
[23]M. E. Lines and E. D. Jones, Phys. Rev. 139, A1313 (1965).
[24]B. A. Coles, J. W. Orton, and J. Owen, Phys. Rev. Lett. 4, 116 (1960).
[25]M. Kohgi, Y. Ishikawa, and Y. Endoh, Solid State Commun. 11, 391 (1972).
[26]M. T. Hutchings and E. J. Samuelson, Solid State Commun. 9, 1011 (1971).
[27]K. Terakura, N. Hamada, T. Oguchi, and T. Asada, J. Phys. F 12, 1661 (1982).
[28]T. Moriya, Prog. Theor. Phys. 33, 157 (1965).
[29]S. Asano and J. Yamashita, Prog. Theor. Phys. 41, 373 (1972).
[30]A. R. Williams, R. Zeller, V. L. Moruzzi, C. D. Gelatt, Jr., and J. Kübler, J. Appl. Phys. 52, 2067 (1981).
[31]L. F. Mattheiss, Phys. Rev. B 5, 290 (1972).
[32]H. A. Alperin, J. Phys. Soc. Jpn. 17, Suppl. B-III, 12 (1962).
[33]J. Kübler (private communication).
[34]F. Ducastelle, J. Phys. C 7, 1795 (1974).